Sawtooth Evolution during JET Ion-Cyclotron-Resonance-Heated Pulses

J. P. Graves and K. I. Hopcraft
School of Mathematical Sciences, University of Nottingham, University Park, Nottingham, NG7 2RD, United Kingdom

R. O. Dendy, R. J. Hastie, and K. G. McClements
EURATOM/UKAEA Fusion Association, Culham Science Centre, Abingdon, Oxfordshire, OX14 3DB, United Kingdom

M. Mantsinen
JET Joint Undertaking, Abingdon, Oxfordshire, OX14 3EA, United Kingdom
(Received 28 May 1999)

The recent Joint European Torus deuterium-tritium campaign has yielded ion-cyclotron-resonance-heated (ICRH) pulses during which both the sawtooth characteristics and the ICRH minority ion population both evolve substantially. At multiple times during each pulse, the evolution of the kinetic-fluid MHD energy is calculated from measurement of the energetic ions and compared with the evolving sawtooth duration. There is strong correlation between sawtooth duration and minority ion stabilization of the ideal internal kink.

PACS numbers: 52.35.Py, 52.50.Gj, 52.55.Fa

Magnetohydrodynamic (MHD) stability of plasmas in the presence of energetic ions is a crucial issue for present and future large tokamak experiments [1,2]. Such ions include 3.5 MeV alpha particles, produced naturally in deuterium-tritium (DT) fusion reactions, and energetic minority species ions produced by ion cyclotron resonance heating (ICRH). A key instability in the plasma core is the sawtooth, which has been observed to move fusion alpha particles radially outwards [3]. However, experiments show [4,5], and theory has predicted [6–8], that it can also be stabilized by ICRH ions. One may ask: first, how reliably the analytical kinetic-fluid theory [9,10] of the ideal $m = n = 1$ internal kink mode provides a quantitative guide to experimental interpretation and prediction of sawtooth stability; and second, how far the consequences of fusion alpha particles for sawtooth stability can be simulated in ICRH experiments not involving radioactive tritium. The conceptual content of these questions is relevant to other naturally occurring plasmas where energetic ion populations couple to MHD activity—for example, in the magnetosphere [11] and supernova remnants [12].

Here we analyze the time-evolving stability properties of recent sawtoothing pulses in the Joint European Torus (JET) [13], subjected to minority hydrogen ICRH [(H)DT and (H)D]. The perturbed kinetic-fluid MHD energy is calculated from measured plasma and energetic ion population parameters at multiple times within each pulse, during which the sawteeth change considerably in character. This goes beyond previous tests [4,5,14] which concentrated on measurements of the threshold ICRH power for sawtooth suppression. Figure 1 shows the time evolution of central electron temperature T_{e0} and ICRH power $P_{\rm rf}$ in four recent JET (H)D and (H)DT pulses; the T_{e0} traces show sawtooth periods τ_s changing by a factor ~ 5 within a single pulse. Each vertical dotted line in Fig. 1 denotes a time at which parameters characterizing the plasma and the energetic ion population were either measured or modeled using the PION code [15], which calculates self-consistently the ICRH power deposition and the energetic ion distribution. The parameter values are used in an extended version of a code [14] which evaluates analytical expressions derived in [9,10,14,16] for the kinetic and fluid contributions of the energetic ions to the perturbed MHD energy. In parallel, and again analytically, a measure of the destabilizing toroidal MHD energy contribution of the plasma at the times shown in Fig. 1 is provided by evaluation of the gradient of the Shafranov shift Δ' for an anisotropic equilibrium [17].

Following [16] we assume $P_{\rm rf} = P_{\rm rf0} \exp[-(R - R_{\rm res})^2/\delta_w^2 - z^2/\delta_v^2]$, where δ_w, δ_v, $R_{\rm res}$ are constants, $R = R_0 + r\cos\theta$, and $z = r\sin\theta$, with R_0, r, and θ denoting, respectively, the major radius, the minor radial distance, and the poloidal angle. We treat $\varepsilon \equiv r/R_0$ as a formal expansion parameter. To leading order, a kinetic treatment indicates that $\partial f_h/\partial\theta|_{\mu,\mathcal{E}} = 0$ [9], where f_h is the hot ion distribution, $\mathcal{E} = v^2/2$, and $\mu = v_\perp^2/2B$, $B = B_0(1 - \varepsilon\cos\theta)$, denoting magnetic induction. A bi-Maxwellian f_h would violate this constraint because of the θ dependence of B [16]. For this reason, we parametrize f_h by hot ion tail temperatures $T_{\perp,h}$ and $T_{\|,h}$ evaluated at the point on the flux surface cross section $\theta = \theta_0$ where heating power is greatest:

$$f_h(r,\mathcal{E},\mu) = \frac{2n_h(r)G(r)}{T_{h,\perp}^{3/2}(r)}\left(\frac{m_h}{2\pi}\right)^{3/2} \times \exp\left[-m_h\left(\frac{\mu B(r,\theta_0)}{2T_{h,\perp}(r)} + \frac{|\mathcal{E} - \mu B(r,\theta_0)|}{2T_{h,\|}(r)}\right)\right], \quad (1)$$

with G a normalization factor [16].

The linear stability of the ideal MHD internal kink mode is often studied using the formalism established in Ref. [18]; toroidal destabilization is controlled by the radial gradient of the Shafranov shift, Δ', evaluated at the $q = 1$ radius. The number of significant poloidal harmonics that couple increases with decreasing aspect ratio; however, the way in which they do so in a highly anisotropic plasma is unclear. Here Δ' is calculated and used to provide a quantitative guide to destabilizing toroidal effects. The pressure tensor $\underline{\underline{P}} = P_{h,\perp}(\underline{\underline{I}} - \hat{\boldsymbol{e}}\hat{\boldsymbol{e}}) + P_{h,\parallel}\hat{\boldsymbol{e}}\hat{\boldsymbol{e}} + P_c\underline{\underline{I}}$, where $\underline{\underline{I}}$ is the unit dyadic, $\hat{\boldsymbol{e}} = \boldsymbol{B}/|B|$, the subscript h denotes "hot," and the subscript c denotes "core," comprising electrons and thermal ions. For experiments encompassing high ICRH power $\lambda(r) = \varepsilon T_{h,\perp}/T_{h,\parallel} \sim O(1)$, thus introducing noncircular distortion of magnetic surfaces in the first order of the equilibrium [17]. Calculating energy moments of Eq. (1) and assuming on-axis heating ($\theta_0 = \pi/2$) gives elements of the pressure tensor,

$$
\begin{aligned}
P_{h,\parallel}(r) &= 2n_h G T_{h,\parallel}(T_{h,\parallel}/T_{h,\perp})^{1/2}, \\
P_{h,\perp}(r,\theta) &= 2n_h G T_{h,\perp}(T_{h,\parallel}/T_{h,\perp})^{1/2}\frac{1}{(1-\lambda\cos\theta)^2} \quad \text{for } \pi/2 < \theta < 3\pi/2, \\
P_{h,\perp}(r,\theta) &= n_h G T_{h,\perp}(T_{h,\parallel}/T_{h,\perp})^{1/2}\left[\frac{(3+\lambda\cos\theta)(\lambda\cos\theta)^{1/2}}{(1+\lambda\cos\theta)^2} + \frac{[1-(\lambda\cos\theta)^{1/2}]^2[(\lambda\cos\theta)^{1/2}+2]}{(1-\lambda\cos\theta)^2}\right] \\
&\qquad \text{for } -\pi/2 < \theta < \pi/2.
\end{aligned}
\tag{2}
$$

Using the above in Eq. (29) of Ref. [17] gives

$$
\Delta' = \varepsilon_1\left[\beta_{pc}(r_1) + \overline{\beta}_{ph}(r_1) + A + \sigma + \frac{1}{4}\right], \tag{3}
$$

where $\Delta' = d\Delta/dr|_{r_1}$, $\varepsilon_1 = r_1/R_0$, $\beta_{pc}(r_1) = -(2\mu_0/R_0^2B_0^2\varepsilon_1^4)\int_0^{r_1} r^2P_c'\,dr$ is the poloidal beta of thermal ions at the singular layer where the safety factor $q(r_1) = 1$, $\overline{\beta}_{ph}(r_1) = -(2\mu_0/R_0^2B_0^2\varepsilon_1^4)\int_0^{r_1} r^2(P_{h,\parallel} + \overline{P}_{h,\perp})'\,dr$, $\overline{P}_{h,\perp} = (1/2\pi)\int_0^{2\pi} P_{h,\perp}\,d\theta$, $A = -(\mu_0/2R_0^2B_0^2\varepsilon_1^4)\int_0^{r_1}(r^2P_{h,\perp}^{(2)})'\,dr$, $P_{h,\perp}^{(2)} = (1/\pi)\times\int_0^{2\pi} P_{h,\perp}\cos(2\theta)\,d\theta$, and $\sigma = (1/r_1^4)\int_0^{r_1} r^3(1/q^2 - 1)\,dr$.

The total plasma pressure affects all core MHD terms of the toroidal energy $\delta W_T \sim \boldsymbol{\xi}\cdot[\boldsymbol{\delta j}\times\boldsymbol{B} + \boldsymbol{j}\times\boldsymbol{\delta B} - \nabla\delta P_i]$, through the Shafranov shift, where δ denotes a perturbation and $\boldsymbol{j}$ is the plasma current. In our ordering of the hot plasma pressure the fast ions contribute only a small correction to Δ'. The remaining term, $\nabla\cdot\underline{\underline{\delta P_h}}$, gives rise to hot fluid and trapped kinetic perturbed potential energies given by Eq. (1) of Ref. [16]:

$$
\begin{aligned}
\delta W_h = &-\frac{1}{2}\int d^3r\left[\boldsymbol{\xi}\cdot\nabla(P_{h,\parallel}+P_{h,\perp}) - (P_{h,\parallel}+P_{h,\perp}+C)\frac{\boldsymbol{\xi}\cdot\nabla B}{B}\right]\frac{\boldsymbol{\xi}^*\cdot\nabla B}{B} \\
&-\frac{1}{2}\int d^3r\int_t d^3\boldsymbol{v}\left(\frac{\omega-\omega_{*h}}{\omega-\langle\omega_{dh}\rangle}\right)|\langle H\rangle|^2\frac{\partial f_h}{\partial\varepsilon},
\end{aligned}
\tag{4}
$$

where ω is the mode frequency, ω_{*h} and $\langle\omega_{dh}\rangle$ are the hot ion diamagnetic frequency and bounce-averaged magnetic drift frequency, respectively, C is defined in Ref. [19], $|\langle H\rangle|^2$ is the bounce-averaged perturbed energy of a trapped particle [9], and t denotes integration over trapped velocity space.

In high power ICRH experiments on JET many minority ions have energies in the MeV range so that $\langle\omega_{dh}\rangle \sim \omega_{*h} \gg |\omega|$, thus the third adiabatic invariant associated with the hot trapped ions is conserved [20]. In this limit the destabilizing fluid effects of hot particles trapped in the region of poor curvature are outweighed by the kinetic effects of trapped ions. The net contribution of trapped ions to δW_h is stabilizing, scaling roughly as $(1 - q - s/2)\beta_h$ [16]. Passing energetic ions also make a stabilizing contribution to the fluid terms in Eq. (4). The analysis in Ref. [16] reduces δW_h to a form suitable for rapid numerical computation; henceforward, we use the normalized potential energy $\delta\hat{W}_h = \delta W_h\mu_0/6\pi^2\xi_0^2R_0B_0^2\varepsilon_1^4$, where ξ_0 is the amplitude of the "top-hat" [21] leading order eigenfunction.

Figure 1 shows that the measured sawtooth period increases with $P_{\rm rf}$. Both $\delta\hat{W}_h$ and Δ' are calculated and plotted in Fig. 2 against the sawtooth free period τ_s, at the times corresponding to the vertical dotted lines in Fig. 1. At each of these times the safety factor is inferred using the EFIT equilibrium reconstruction code [22], and at the times corresponding to the dotted lines the value of q on the axis typically decreases from 0.8 early in the discharge to 0.7 later on, while the $q = 1$ radius r_1/a typically increases from 0.2 to 0.4. In addition, the electron temperature and thermal ion temperature profiles are measured, and the rf heating position and hot ion tail temperatures are calculated [15]. This enables $\beta_{pc}(r_1)$ and $\overline{\beta}_{ph}(r_1)$ to be inferred: at the times corresponding to the dotted lines,

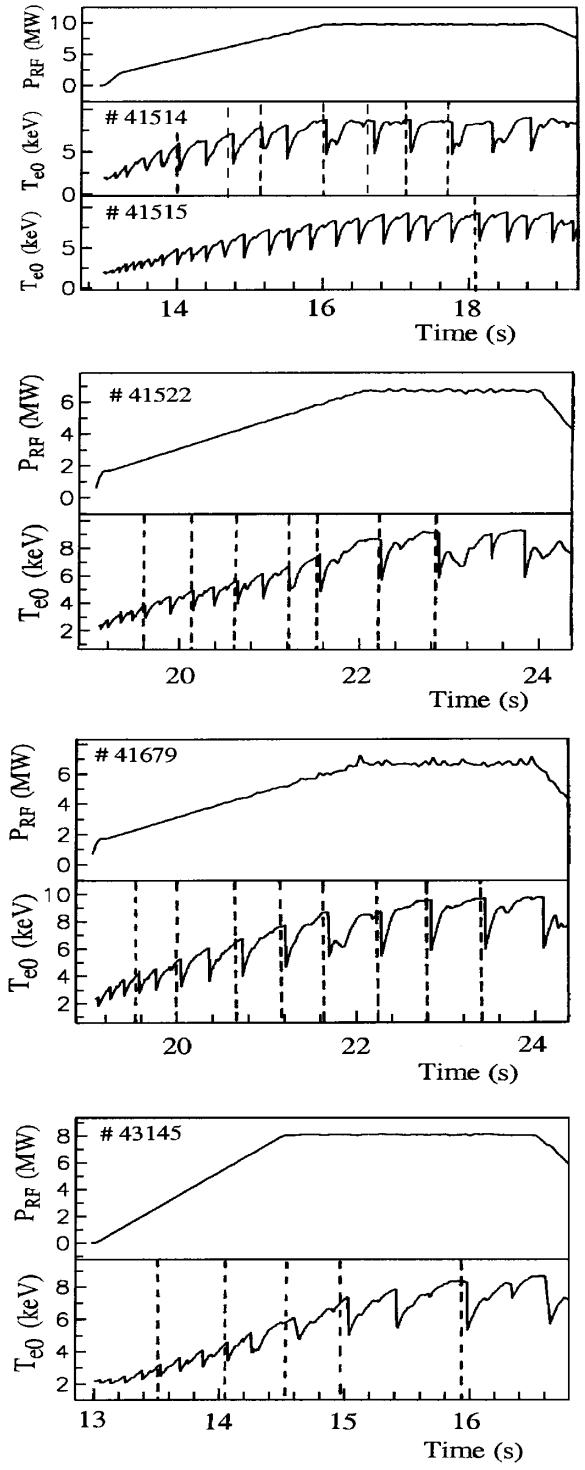

FIG. 1. Time profiles of ICRH power and central electron temperature. Discharges 43145, 41514, 41515, and 41522 are (H)D plasmas. Discharge 41679 is a (H)DT plasma. Vertical dotted lines correspond to times of internal kink calculations (see Fig. 2).

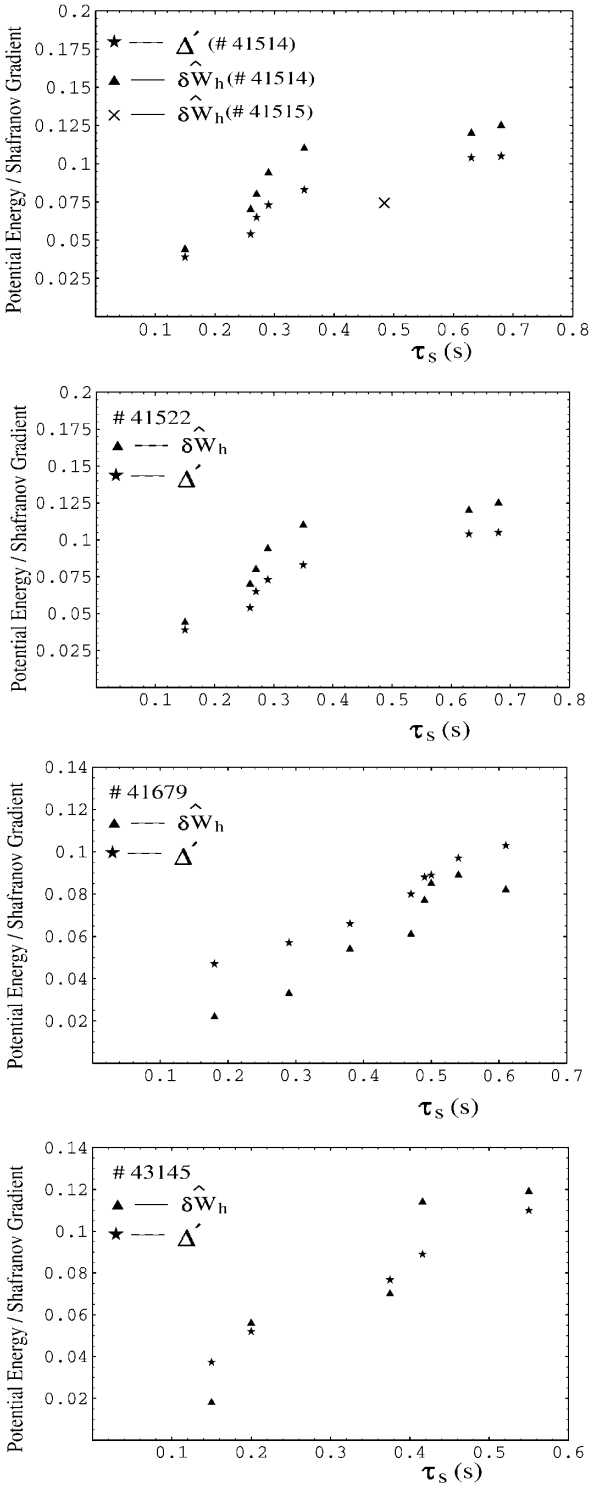

FIG. 2. Computed values of Δ' and $\delta\hat{W}_h$ and measured values of sawtooth duration τ_s at multiple times during the discharges shown in Fig. 1.

these typically increase from 0.09 (early) to 0.15 (later) and from 0.05 to 0.15, respectively. Other quantities such as the plasma density n_e are approximately constant throughout the discharges.

Figure 2 demonstrates that in five separate JET pulses the stabilizing effects associated with energetic particles and the destabilizing effects of higher pressure both increase with lengthening sawtooth period. Theory suggests [6–8] that, as the plasma pressure rises and Δ' increases

during a pulse, continued stabilization is possible if $\delta\hat{W}_h$ increases sufficiently. Thus, the systematic correlation between $\delta\hat{W}_h$, Δ', and τ_s throughout Fig. 2 is consistent with the premise that a sawtooth crash occurs when the ideal kink mode is close to marginal stability. This is clear in pulses 41522, 41679, and 43145 and additional support is provided by pulses 41514 and 41515. The latter are identical, except that the rf wave orientation was reversed. As a result the perpendicular tail temperature of ions in 41514 peaked at 850 keV, but only at 350 keV in 41515 [23]. The sawteeth in 41514 are of a much longer duration than those of 41515, thus providing additional evidence for sawtooth stabilization by populations of energetic ions. Contrasting levels of stabilization from the energetic ions, quantified by calculating $\delta\hat{W}_h$ during pulses 41514 and 41515, are shown in Fig. 2: data for energetic ions in 41515 were available only at a single time.

We have not so far considered resistive effects on $m = 1$ mode stability. It can be shown [6–8] that these are controlled by a parameter $\Lambda \equiv -i[\omega(\omega - \hat{\omega}_{*e})(\omega - \omega_{*i})]^{1/3}/\gamma_R$, where $\hat{\omega}_{*e} = \omega_{*e}(1 + 0.71\eta_e)$, $\omega_{*e} = (dP_e/dr)/(en_eB_0r)$, $\omega_{*i} = -(dP_i/dr)/(en_eB_0r)$, $\eta_e = d\ln T_e/d\ln n_e$ and γ_R is the growth rate of the resistive $m = 1$ mode. This last quantity varies as $s_1^{2/3}$, where s_1 is magnetic shear at the $q = 1$ surface. The ideal limit is represented by $|\Lambda| \to \infty$. Solving the full resistive dispersion relation [6–8] could, in principle, enable us to carry out further comparisons with observation. In practice, uncertainties in the q profile preclude meaningful comparisons: in particular, the transition between ideal and resistive behavior is controlled by the value of Λ, which itself is strongly dependent on s_1, a parameter which could not be measured directly in the JET pulses considered here.

In summary, the JET DTE1 campaign included sawtoothing ICRH pulses in which both the sawtooth characteristics and the energetic minority ion population evolved substantially. For multiple times during several sawtoothing pulses, the evolution of the kinetic–fluid MHD energy has been calculated from measurements and PION simulations of the energetic ions, and compared with the evolving sawtooth duration. We have shown that minority ion stabilization of the $m = 1$ internal kink mode increases in parallel with destabilizing toroidal effects, as expected from experimental observations of increasing sawtooth duration. This is consistent with previous demonstrations that q_0 usually remains below unity for the whole sawtooth period in JET [24]. Despite this, long ramping times and giant sawteeth are observed, the latter coinciding with strong kinetic stabilization. The consistency of our stability calculations with sawtooth behavior during each pulse enhances confidence in the applicability of the kinetic–fluid energy principle [9,10] to modeling and predicting sawtooth phenomenology in present and future tokamak fusion experiments involving energetic particles.

We are grateful to the late David Start for assistance, and thank the JET team for providing data from sawtoothing discharges. This work was carried out under a Task Agreement between UKAEA and JET and funded in part by the Engineering and Physical Sciences Research Council, the U.K. Department of Trade and Industry, and Euratom.

[1] R. Hawryluk, Rev. Mod. Phys. **70**, 537 (1998).
[2] F. Porcelli, D. Boucher, and M. N. Rosenbluth, Plasma Phys. Controlled Fusion **38**, 2163 (1996).
[3] M. P. Petrov *et al.*, Nucl. Fusion **35**, 1437 (1995).
[4] D. Campbell *et al.*, Phys. Rev. Lett. **60**, 2148 (1988).
[5] C. K. Phillips *et al.*, Phys. Fluids B **4**, 2155 (1992).
[6] R. B. White *et al.*, Phys. Rev. Lett. **60**, 2038 (1988).
[7] R. B. White, M. N. Bussac, and F. Romanelli, Phys. Rev. Lett. **62**, 539 (1989).
[8] B. Coppi *et al.*, Phys. Rev. Lett. **63**, 2733 (1989).
[9] T. M. Antonsen and Y. C. Lee, Phys. Fluids **24**, 1465 (1981).
[10] L. Chen, R. B. White, and M. N. Rosenbluth, Phys. Rev. Lett. **52**, 1122 (1984).
[11] J. R. Johnson and C. Z. Cheng, J. Geophys. Res. **102**, 7179 (1997).
[12] B. R. Ragot and J. G. Kirk, Astron. Astrophys. **327**, 432 (1997).
[13] JET Team, M. Keilhacker *et al.*, Plasma Phys. Controlled Fusion **39**, B1 (1997).
[14] K. G. McClements *et al.*, Phys. Plasmas **3**, 2994 (1996).
[15] L.-G. Eriksson, T. Hellsten, and U. Willén, Nucl. Fusion **33**, 1037 (1993).
[16] R. O. Dendy *et al.*, Phys. Plasmas **2**, 1623 (1995).
[17] N. A. Madden and R. J. Hastie, Nucl. Fusion **34**, 519 (1994).
[18] M. N. Bussac *et al.*, Phys. Rev. Lett. **35**, 1638 (1975).
[19] J. B. Taylor and R. J. Hastie, Phys. Fluids **8**, 323 (1965).
[20] F. Porcelli, Plasma Phys. Controlled Fusion **33**, 1601 (1991).
[21] V. D. Shafranov, Sov. Phys. Tech. Phys. **15**, 175 (1970).
[22] L. L. Lao *et al.*, Nucl. Fusion **30**, 1035 (1990).
[23] L.-G. Eriksson *et al.*, Phys. Rev. Lett. **81**, 1231 (1998).
[24] J. Blum *et al.*, Nucl. Fusion **30**, 1475 (1990).